A van der Waals density functional study of the adsorption of ethanol on the α-alumina (0001) surface

Karen Johnston

Department of Chemical and Process Engineering, University of Strathclyde, Royal College Building, 204 George Street, Glasgow G1 1XW, United Kingdom
Email: karen.johnston@strath.ac.uk
Tel: +44 141 548 2837

Abstract

The interaction of an ethanol molecule with an α-alumina (0001) surface is investigated using density functional theory. The adsorption structure, adsorption energy, partial charges and charge densities of various non-dissociated and one dissociated structure were calculated. The results obtained using a generalised gradient approximation (GGA) functional, and three different van der Waals (vdW) functionals were compared. For every structure, the GGA functional gave the smallest adsorption energy. The vdW functionals for each structure gave adsorption energies about 0.3-0.4 eV larger than the GGA functional, but the energetic ordering of the structures remained mostly the same with the exception of only a few almost degenerate non-dissociated structures. The dissociated structure was found to be energetically the most favorable with an adsorption energy ranging from 1.33 to 1.84 eV, depending on the functional. This is around 0.1 eV more strongly bound than the lowest energy non-dissociated structure.

The adsorption of organic molecules on inorganic surfaces is of growing interest in many applications including catalysis, self-assembled monolayers and biomineralisation, to name a few examples. For example, the adsorption of small alcohol molecules on oxide surfaces is of interest in morphological control of crystal growth, such as in biomineralisation[1, 2]. Another example where alcohol adsorption is important is in polymer coatings. Polyurethane protective coatings are applied to a metal (oxide) surface as a mixture of dialcohols, trialcohols and dicyanates which polymerize in situ. If some of these molecules bond to the surface or more readily interact with the surface than others then the composition of the polymer coating may not be uniform, which may impair adhesion to the surface.

Preprint submitted to Elsevier *August 30, 2013*

While there are several studies of ethanol on oxide surfaces, such as strontium titanate [3], zinc oxide [4] and γ-alumina [5], there are not many studies on clean α-alumina. Computational studies of the dehydrogenation of ethanol on alumina have focused on the catalytic surfaces 3Niα-Al_2O_3 [6] and 2Rhγ-Al_2O_3 [7]. Studies of phenol on α-Al_2O_3 [8] and methanol on α-Al_2O_3 [9] focused only on the non-dissociated structures. *Ab initio* studies of water on alumina have shown that both dissociated and non-dissociated structures co-exist [10, 11, 12]. Experimental studies of methanol on alumina have observed only molecular adsorption on clean α-alumina [13, 14, 15] whereas inelastic electron tunneling spectroscopy observed that ethanol dehydrogenates to form an ethoxide on the surface [16]. An infrared study observed a weakly bound layer of liquid ethanol at 35 ^{o}C in addition to the ethoxide [17]. This weakly bound layer is likely to be non-dissociated precursor states for the dissociation. However, the alumina surface was not well characterised in this early work and only in the last decade detailed experimental results about the various surface structures have become available.

In this work non-dissociative and dissociative structures of an ethanol molecule with the α-Al_2O_3 surface are investigated. In density functional theory (DFT), the generalised gradient approximation (GGA) for the exchange and correlation functional does not include the effects of van der Waals (vdW) forces and for this reason vdW forces have often been neglected in DFT studies of adsorption. However, with the recent development of various methods that take vdW forces into account in DFT calculations [18, 19, 20, 21], many low density (molecular) systems that were previously not suitable for DFT studies can now be studied. Many of these methods have been tested on the S22 set of molecular systems and the exchange functional can have a significant effect on the energies [19, 20, 22]. vdW forces have a significant effect on polarizable materials, such as benzene on gold [23, 24], and also in systems where the molecules are chemically bonded to the surface, such as benzene or phenol on silicon [25, 26, 27, 28]. However, the importance of vdW interactions on molecular adsorption on oxide surfaces and the difference between the results using different functionals have not been thoroughly investigated. In this work, several exchange and correlation functionals are used to investigate various adsorption structures of ethanol on alumina and the energetics and electronic structures obtained using the different functionals are compared. The organisation of the paper is as follows. In the following section, the details of density functional calculations are described. The bulk and surface properties of alumina are calculated using four different exchange and correlation functionals and the results are compared to previous literature. The binding energies and prop-

erties of a range of non-dissociated structures of ethanol and one dissociated structure are presented.

1. Method

The density functional theory calculations were performed using the VASP code [29, 30]. The core electrons were described using projector augmented waves (PAW) [31, 32] and for the valence electrons a planewave energy cutoff of 500 eV was used. Four different exchange and correlation functionals were used: a standard generalised gradient approximation (PBE) [33, 34, 35], the vdW-DF functional with the original revPBE exchange [18, 19], vdW-DF with PBE exchange (denoted vdW-DF*) and vdW-DF2, which is similar to vdW-DF but has a more accurate kernel and uses PW86 exchange [21].

The lowest energy stoichiometric alumina surface is terminated by a single layer of Al atoms [36, 37], as shown in Fig. 1. This slab has 30 atoms in the surface unit cell, corresponding to 18 atomic layers. The bottom six atomic layers are held fixed and the slab was relaxed until the maximum force on the ions was less than 10 meVÅ^{-1}. The surface and bulk calculations used a Brillouin zone mesh of $4\times4\times1$, centred on the Γ-point. For the adsorption studies, the cell height was around 40 Å corresponding to a vacuum layer of approximately 27 Å. For all calculations a dipole correction was applied in the z-direction. A coverage of one monolayer is defined as one molecule per surface unit cell and for a 0.25 monolayer coverage of ethanol on alumina considered here a Γ-centred Brillouin zone mesh of $2\times2\times1$ was used. Partial charges were calculated using the Bader analysis method [38, 39, 40].

2. Results and Discussion

2.1. Bulk and surface properties of alumina

While the vdW functionals have been shown to give excellent results for molecule-molecule interactions, there are only a few studies on solids and heterogeneous systems [41, 42]. Therefore, before using these functionals to study the interaction of molecules on an alumina surface, the properties of bulk alumina and the studied surfaces were calculated and compared with standard GGA and experimental results. Here, the values for the 30-atom hexagonal lattice for alumina, which contains three primitive cells, are reported. The bulk lattice constant calculated by PBE is 4.81 Å, which is 1.1% larger than the experimental lattice constant (extrapolated to T=0 K)

of 4.76 Å and is a typical result for GGA calculations. The vdW-DF functional overestimates the lattice constant by 1.7% compared to experiment but using PBE exchange improves this slightly to 1.3%. A similar trend was seen for other oxides[43, 41], where vdW-DF (with revPBE exchange) overestimates the lattice constants more than the vdW-DF functional with PBE exchange or optPBE exchange. The lattice constant predicted by the vdW-DF2 functional is rather worse than vdW-DF and overestimates the experimental value by 2.1%. However, the c/a ratio and the atomic displacements Δx_{O} and Δx_{Al} are similar in each case. The values are reported in Table 1.

The relaxed surface is shown in Fig. 1. It can be seen that the top Al atoms move inwards from the surface to become coplanar with the O atoms, which minimises the surface dipole. The interlayer spacings are presented in Table 1. The PBE interlayer spacings are in good agreement with previous work that used generalised gradient approximations for exchange and correlation functional [36, 37, 9]. The three vdW functionals predict a slightly smaller inwards relaxation of the top Al atoms of −74% to −80%, which agrees better with an experimental value of −63% [46] than the standard GGA functionals, which predict a relaxation of −84% to −86% [36, 37, 9]. All other interlayer displacements are similar to the PBE results.

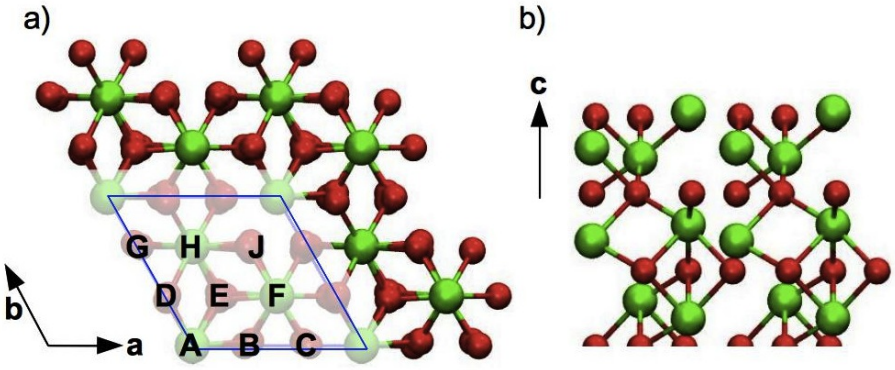

Figure 1: a) Top and b) side views of the alumina surface. Al and O atoms are represented by green and red spheres, respectively. The blue parallelogram in a) is the surface unit cell.

The partial charges for the atoms in the top six atomic surface layers and also the partial charges of the ethanol molecule have been calculated and the results are compared in Table 1. For the alumina surface, the partial charges are very similar for all functionals. In the isolated ethanol molecule

Table 1: Comparison of various exchange and correlation functionals for lattice constants and structural parameters for bulk alumina, structural relaxations of the isolated alumina surface and partial charges of the isolated alumina surface and ethanol molecule.

Properties of bulk α-alumina							
	PBE	vdW-DF	vdW-DF*	vdW-DF2	Expt[44]		
a(Å)	4.81	4.84	4.82	4.86	4.76		
c/a	2.73	2.73	2.73	2.73	2.73		
Δx_{O}(Å)	0.3061	0.3065	0.3063	0.3064	0.3062		
Δx_{Al}(Å)	0.1478	0.1476	0.1476	0.1471	0.1478		
Percent change in interlayer spacing							
Layer	PBE	vdW-DF	vdW-DF*	vdW-DF2	PW91[36]	GGA[37]	PW91[9]
1 Al–O_3	−86	−80	−74	−76	−86	−84	−85
2 O_3–Al	0	+4	+2	+4	+6	+17	+4
3 Al–Al	−38	−49	−39	−44	−49	−58	−46
4 Al–O_3	+19	+20	+17	+20	+22	–	+19
5 O_3–Al	+5	+5	+4	+4	+6	–	–
6 Al–Al	−8	−14	−6	−6	–	–	–
Partial charges of top 6 atomic layers of alumina surface (e)							
Atom	PBE	vdW-DF	vdW-DF*	vdW-DF2	HF[45]		
Al	+2.42	+2.43	+2.42	+2.42	+1.91		
O	−1.63	−1.64	−1.63	−1.63	−1.66		
Al	+2.48	+2.50	+2.49	+2.49	–		
Al	+2.49	+2.50	+2.50	+2.50	–		
O	−1.66	−1.67	−1.67	−1.67	–		
Al	+2.48	+2.50	+2.49	+2.49	–		
Partial charges of isolated ethanol molecule (e)							
Atom	PBE	vdW-DF	vdW-DF*	vdW-DF2	LDA[39]		
C_{OH}	+0.45	+0.45	+0.46	+0.45	+0.42		
C_{H_3}	−0.03	+0.07	+0.04	+0.08	−0.08		
O	−1.11	−1.07	−1.08	−1.07	−1.05		
H_O	+0.59	+0.56	+0.56	+0.56	+0.55		
$H_{C_{OH}}$	+0.02	0.00	0.00	0.00	+0.03		
$H_{C_{H_3}}$	+0.02	0.00	+0.01	−0.01	+0.04		

the three equivalent H atoms in the CH_3– group are denoted by $H_{C_{H_3}}$, the two equivalent H atoms in the –CH_2OH group are denoted by $H_{C_{OH}}$ and the H attached to the O is denoted by H_O. For ethanol there are only small differences, the main difference being that the oxygen atom is predicted to

be slightly less negative by $0.04e$ using the vdW functionals and the H_O atom is, correspondingly, $0.03e$ less positive.

2.2. Adsorption structure and energy of ethanol on alumina

The adsorption energy is defined as

$$E_{\mathrm{ads}} = E_{\mathrm{srf}} + E_{\mathrm{mol}} - E_{\mathrm{tot}}$$

where E_{srf} is the energy of the clean surface, E_{mol} is the energy of the isolated molecule and E_{tot} is the total energy of the molecule adsorbed on the surface. Since there are likely to be many local minima for non-dissociative adsorption, a series of initial configurations for ethanol were set up by placing ethanol on the various adsorption sites, which are labelled in Fig. 1a. The position (site) of the ethanol is defined using the centre of geometry of the two C atoms. The angle that the C–C bond makes with the surface plane is denoted by θ, so that $\theta = 0°$ corresponds to horizontal orientations. An angle of $\theta = -90°$ means that the C–C bond is perpendicular to the surface with the –OH group towards the surface. For the flat configurations, where the C–C bond is aligned parallel to the surface, ϕ is defined as the angle in the surface plane between the C–C bond and the a-axis. The x and y coordinates of the carbon atoms were kept fixed. All initial horizontal configurations had the –OH group pointing towards the surface, since the electrostatic attraction between the –OH group and the Al and O surface ions is expected to give lower adsorption energies. In addition to the horizontal configurations, two vertical configurations with $\theta = -90°$, corresponding to the –OH group pointing towards the surface, and one vertical configuration with $\theta = 90°$, corresponding to the –OH group pointing away from the surface, were investigated. For $\theta = 90°$ only one site was considered since the CH_3 group is not expected to have a strong electrostatic interaction with the surface. For $\theta = -90°$, two configurations of ethanol were considered, one on site A and the other on site E. The adsorption energies for all of these configurations using the various functionals are presented in Table 2.

First, the results for the various structures using the PBE functional are discussed. From the energies in Table 2, it can be seen that the non-dissociated horizontal structures have a range of adsorption energies from almost 0.23 eV (site G) up to 1.26 eV (site J). There is a correlation between adsorption energy and the distance between the ethanol oxygen atom and the closest surface Al atom. The configuration on site J has the largest adsorption energy since this site enables the the ethanol oxygen atom to

Table 2: Adsorption energy (eV) for various configurations of ethanol on the alumina surface. Configurations are ordered from low to high PBE adsorption energy.

Site	θ (°)	ϕ (°)	PBE	vdW-DF	vdW-DF*	vdW-DF2
A	90	–	0.01	0.23	0.32	0.24
G	0	0	0.23	0.49	0.67	0.57
C	0	0	0.26	0.46	0.65	0.54
A	-90	–	0.29	0.50	0.76	0.60
D	0	0	0.53	0.67	0.97	0.79
H	0	0	0.55	0.72	0.99	0.82
A	0	0	0.55	0.73	1.01	0.83
F	0	0	1.03	1.17	1.40	1.25
B	0	0	1.04	1.49	1.51	1.33
E	0	0	1.08	1.34	1.58	1.43
E	-90	–	1.21	1.40	1.64	1.49
J	0	0	1.26	1.49	1.76	1.59
Dissociated			1.33	1.60	1.84	1.73

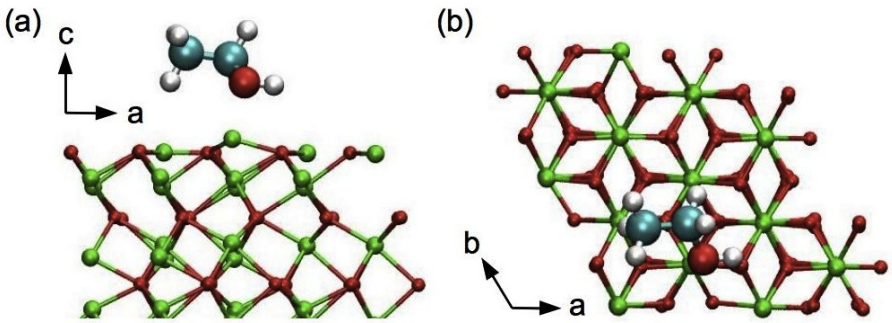

Figure 2: (a) Side and (b) top view of the relaxed structure of ethanol on site J. The ethanol oxygen atom is attracted to the Al atom on site F, which is pulled up from the surface.

be close to the surface Al atom at site F, as shown in Fig. 2. The vertical configuration with $\theta = -90°$ on site E also has a large adsorption energy of 1.21 eV, which is also due to the interaction between the -OH group and the surface Al atom at site F. The vertical configuration with $\theta = -90°$ on site A, does not permit the oxygen to approach a surface Al atom and, instead a hydrogen bond between the H atom and a surface oxygen atom is formed and the configuration has a low adsorption energy of 0.26 eV, which is a

typical energy for a hydrogen bond. The vertical configuration with $\theta = 90°$ on Site A, where the –OH group is pointing away from the surface, exhibits almost no attractive interaction. The energy of structure J of 1.26 eV is very similar to the GGA-PW91 result of the non-dissociative adsorption of methanol on α-alumina, which has an adsorption energy of 1.23 eV [9]. It is also comparable to phenol on α-alumina, which has an adsorption energy of 1.00 eV, using GGA-PW91 [47]. A lower adsorption energy of 0.66 eV was calculated for phenol on α-alumina using the GGA-revPBE functional [8]. A similar difference between revPBE and PBE adsorption energies has been reported in a study of phenol on silicon [27].

Next, the results from different exchange and correlation functionals will be compared. For every configuration, PBE gives the smallest adsorption energy of all the functionals. A quantitative comparison between PBE and vdW-DF*, which uses PBE for exchange, shows that the vdW-DF* adsorption energy ranges from about $0.3 - 0.5$ eV larger than for PBE. This is a large difference but, in general, the energetic ordering of all the configurations is similar, the exception being structures C and G, whose ordering is reversed for the vdW functionals, compared to PBE. However, the difference in adsorption energy between C and G is small for all functionals (not more than 0.03 eV). For all configurations vdW-DF* gives the highest adsorption energy of all the functionals. The adsorption energies for vdW-DF are about $0.15 - 0.25$ eV larger than the values obtained using PBE, which is consistent with the findings for phenol on alumina [47], with the exception of configuration B, where the energy is 0.45 eV larger. This exception is not an effect of the functional but is due to the fact that a different relaxed structure has been found, which will be discussed below. vdW-DF2 is about 0.1 eV larger than vdW-DF for all horizontal configurations, except for A90, where the energies are approximately equal. For this structure the PBE adsorption energy is negligible and the weak interaction is almost purely due to vdW forces. The similarity in the energies for A90 is, therefore, not surprising since the three vdW functionals are very similar. Overall, there is a rather large range in adsorption energies of up to 0.5 eV for the different functionals, which can be mainly attributed to the differences in exchange.

The behavior of the functionals is further compared by looking at the dependence of the binding energy on the distance from the surface for the configuration J. Configuration J was fully relaxed by removing the constraints on the x and y coordinates of the C atoms. The adsorption energy of the relaxed structure increased by only $0.01 - 0.02$ eV for all functionals. Starting from the minimum energy structure the molecule was rigidly moved along the z-direction, with neither the molecule nor the surface relaxed further.

The adsorption distance, z_{ads}, is defined as the distance, perpendicular to the surface plane, from the midpoint of the C–C bond to the top Al surface atom, as shown in the inset of Fig. 3. The results of this calculation for each functional are shown in Fig. 3. The position of the minimum for the vdW-DF functional is almost the same as for the PBE functional. The other two vdW functionals have slightly smaller minimum positions. These differences do not appear to be systematic since a study of benzene physisorbed on tin dioxide[48] showed that the adsorption distance predicted by vdW-DF* is larger than for vdW-DF.

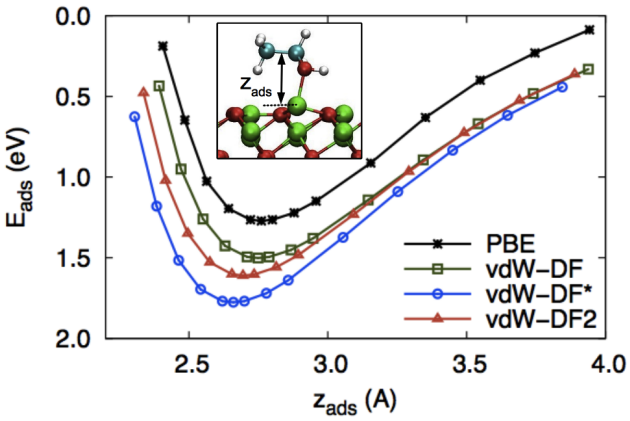

Figure 3: Adsorption energy as a function of z on site J for the various functionals. The inset shows the configuration for the PBE functional and the adsorption distance is labelled.

Now, the structural properties of the lowest energy non-dissociated structure, configuration J, will be described in more detail and the results are compared to previous work on non-dissociated methanol on α-alumina[9]. The distance between the ethanol oxygen and surface aluminum, $d_{\mathrm{O_{eth}-Al}}$, is between $1.93 - 1.95$ Å, for the different functionals, which is in excellent agreement with the 1.93 Å found for methanol on alumina. As mentioned previously, it is the closeness between the O atom and Al atom that is the main reason for the strong adsorption energy of this configuration. The relaxed structure is shown in Fig. 2 and it can be seen that this surface aluminum atom is pulled up from the surface. The perpendicular distance from the Al to the average surface oxygen atoms, $z_{\mathrm{Al-O_s}}$, is $0.43 - 0.44$ Å, which also agrees with methanol on alumina. The angle that the C–O bond makes with the surface normal, denoted ϕ_{COz}, is 58° using PBE, which com-

9

pares well with the corresponding angle for methanol adsorption of 57°. The various quantities are presented in Table 3.

Table 3: Structural information for ethanol non-dissociated on site J and site B of the alumina surface and the dissociated structure. Distances are in Å and angles are in degrees. Ref. [9] is methanol physisorbed on alumina using the PW91 GGA functional.

J	PBE	vdW-DF	vdW-DF*	vdW-DF2
$d_{O_{eth}-Al}$	1.93	1.95	1.93	1.95
$d_{H_{OH}-O_s}$	2.29	2.40	2.34	2.35
z_{Al-O_s}	0.44	0.43	0.43	0.43
ϕ_{COz}	58	60	62	62
B	PBE	vdW-DF	vdW-DF*	vdW-DF2
$d_{O_{eth}-Al}$	1.96	1.95	1.97	1.98
$d_{H_{OH}-O_s}$	1.91	2.42	1.94	1.98
z_{Al-O_s}	0.47	0.43	0.46	0.46
ϕ_{COz}	34	59	36	35
Dissociated	PBE	vdW-DF	vdW-DF*	vdW-DF2
$d_{O_{eth}-Al}$	1.71	1.73	1.72	1.73
$d_{H_{OH}-O_s}$	0.98	0.98	0.98	0.98
z_{Al-O_s}	0.75	0.74	0.73	0.74
ϕ_{COz}	50	52	53	54
	Methanol PW91[9]	Phenol PW91[47]	Phenol revPBE[8]	
$d_{O_{mol}-Al}$	1.93	1.95	-	
$d_{H_{OH}-O_s}$	2.03	-	-	
z_{Al-O_s}	0.43	-	-	
ϕ_{COz}	57	44.7	42.4	

The same analysis has been applied to configuration B for all the functionals in order to elucidate the anomalously high adsorption energy predicted using vdW-DF. The PBE and vdW-DF structures are shown in Fig. 4 and the data is presented in Table 3. From Fig. 4 it is clear that for the vdW-DF functional the –OH group of the ethanol has rotated so that the oxygen is close to the surface Al on site F. This structure now roughly mirrors configuration J, which is clearly seen from the data for B with vdW-DF, which is almost identical to the structural data for configuration J.

For the dissociated structure the O–H bond of the ethanol is broken and the CH_3CH_2O- and H- radicals bond to surface Al and O atoms, respectively,

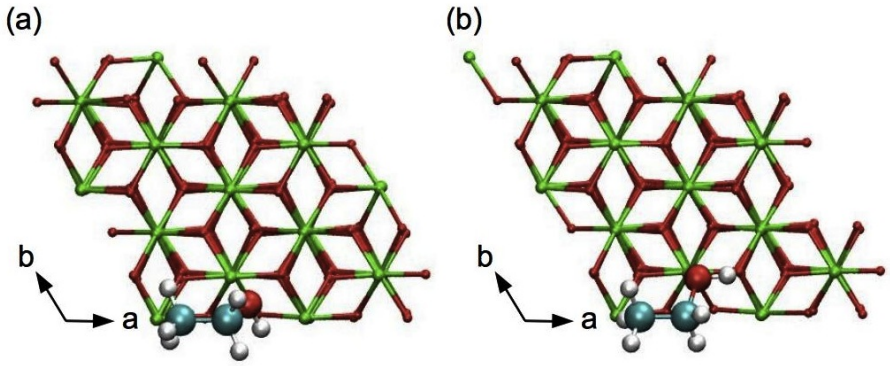

Figure 4: Top view of ethanol on site B using (a) PBE and (b) vdW-DF. In (b) the ethanol oxygen atom is closer to the Al atom on site F and the hydrogen atom has rotated so that the O–H bond is along the a-axis.

as shown in Fig. 5. Since the bond between the Al atom and one of the neighbouring surface O atoms is also broken, the Al moves outward from the plane of O atoms. A similar adsorption structure has been observed for methanol and phenol on α-alumina(0001) [9, 47, 8]. The adsorption energy

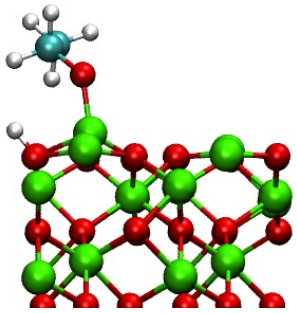

Figure 5: Dissociative adsorption on the alumina surface. Al, O, C and H atoms are represented by green, red, blue and white spheres, respectively.

of the dissociated structure is between 0.07 and 0.14 eV higher than the adsorption energy of configuration J for all functionals. This small energetic difference implies that both non-dissociated and dissociated molecules could be present on the surface of alumina in support of experimental observations [17, 16]. However, this also depends on the barrier required to sever the OH bond. In addition, zero point vibrational corrections are neglected.

The adsorption energies using the PBE functional are slightly lower than the adsorption energy of 1.84 eV (42.58 kcal mol^{-1}) of non-dissociated ethanol on γ-alumina found by Wu *et al.* using the PW91 [49] GGA functional [7]. Similar to the current results, they found that the –OH group bonds to a low-coordinated Al atom.

2.2.1. Partial charges and charge density

The Bader partial charges for ethanol on site J are given in Table 4. The equivalence of the $H_{C_{H_3}}$ atoms in the molecule has been broken and there is a difference between the atoms pointing towards the surface and pointing away from the surface. The two H atoms pointing away from the surface are denoted by $H^{u}_{C_{H_3}}$ and the H atom closest to the surface is denoted by $H^{d}_{C_{H_3}}$. Similarly, for the $–CH_2OH$ group, the atoms nearest and furthest from the surface are denoted by $H^{d}_{C_{OH}}$ and $H^{u}_{C_{OH}}$, respectively. For the PBE functional the C_{OH} atom is less positively charged by around $0.15e$ than for the isolated ethanol molecule, which is given in Table 1. For the isolated molecule the partial charge on the C_{OH} varies by only $0.01e$ for the different functionals but for the adsorbed molecule the partial charge varies by up to $0.10e$, with the vdW functionals giving a more positive charge than PBE. For vdW-DF2 the charge is 0.40, which is only $0.05e$ smaller than for the isolated molecule. Despite these differences in the Bader charges the molecule remains neutral and there is no charge transfer between the surface and the molecule.

For the surface Al atom closest to the ethanol oxygen, adsorption leads to a very slight increase in charge of $+0.02e$ to $+0.04e$ for the various functionals compared to the clean surface. The difference in the partial charges of the surface oxygen atoms between the clean and adsorbed surfaces was less than $0.01e$. This last result is in contrast to the results of methanol on alumina, where no change in partial charge of the Al atom close to the ethanol oxygen was seen, whereas the surface oxygen close to the hydroxyl H atom was seen to lose $0.04e$ to $0.06e$ [9].

The Bader charges for the dissociated structure are given in Table 5. For the dissociated structure, the C_{OH} atom is more positively charged than in the isolated molecule and the O atom is more negatively charged. PBE predicts an increase of $0.04e$ and the largest increase of $0.14e$ is predicted by vdW-DF. The total charge transfer to the ethanol molecule is $-0.17e$, $-0.22e$, $-0.20e$ and $-0.25e$ using PBE, vdW-DF, vdW-DF* and vdW-DF2, respectively. This charge transfer is mainly coming from the alumina oxygen atom that is bonded to the dissociated H atom, denoted by O_H, which increases from around $-1.6e$ in the isolated alumina slab to around $-1.45e$.

12

Table 4: Partial charges for ethanol on site J calculated using the various exchange and correlation functionals.

Atom	PBE	vdW-DF	vdW-DF*	vdW-DF2
Al_{eth}	+2.44	+2.46	+2.45	+2.46
Al	+2.42	+2.43	+2.41	+2.41
O	−1.62	−1.64	−1.63	−1.63
Al	+2.47	+2.49	+2.48	+2.28
Al	+2.48	+2.50	+2.49	+2.49
O	−1.66	−1.66	−1.66	−1.66
Al	+2.47	+2.48	+2.48	+2.48
C_{OH}	+0.30	+0.35	+0.34	+0.40
C_{H_3}	−0.11	+0.04	+0.03	+0.04
O	−1.23	−1.19	−1.19	−1.18
H_O	+0.66	+0.63	+0.62	+0.62
$H^d_{C_{OH}}$	+0.12	+0.08	+0.08	+0.08
$H^u_{C_{OH}}$	+0.05	+0.02	+0.04	−0.02
$H^d_{C_{H_3}}$	+0.12	+0.07	+0.08	+0.07
$H^u_{C_{H_3}}$	+0.05	0.00	0.01	0.01
$H^u_{C_{H_3}}$	+0.04	+0.01	−0.01	−0.02

To understand better how the charge is reorganised in the system, one can look at the difference between the electronic charge density profiles of the adsorbed and isolated states at position r, which is defined as

$$\Delta\rho(r) = \rho_{\mathrm{tot}} - \rho_{\mathrm{srf}} - \rho_{\mathrm{mol}}$$

where ρ_{srf} and ρ_{mol} are the charge densities of the isolated surface and molecule, respectively, but with the same ionic coordinates as the total adsorbed system. To obtain a 1-D representation of the difference in charge densities, $\rho(r)$ can be averaged over the xy-plane to give a profile along the z-direction, $\rho(z)$, defined as

$$\rho(z) = \int\int \rho(r)\ \mathrm{d}x\,\mathrm{d}y$$

which can then be used to calculate the charge difference profiles

$$\delta\rho(z) = \rho_{\mathrm{tot}}(z) - \rho_{\mathrm{srf}}(z) - \rho_{\mathrm{mol}}(z).$$

The charge density difference for the non-dissociated structure on site J using the PBE functional, is shown in Fig. 6(a). There are charge accumulation regions (blue) around the oxygen atom of the ethanol and above the top

13

Table 5: Partial charges for the dissociated adsorption structure of ethanol.

Atom	PBE	vdW-DF	vdW-DF*	vdW-DF2
Al_{eth}	+2.46	+2.47	+2.46	+2.46
Al	+2.42	+2.43	+2.42	+2.41
O_H	−1.49	−1.48	−1.48	−1.45
O	−1.62	−1.63	−1.64	−1.63
Al	+2.47	+2.49	+2.48	+2.48
Al	+2.48	+2.49	+2.49	+2.49
O	−1.66	−1.66	−1.66	−1.66
Al	+2.47	+2.48	+2.48	+2.48
C_{OH}	+0.49	+0.59	+0.53	+0.56
C_{H_3}	−0.08	−0.02	+0.03	+0.05
O	−1.35	−1.36	−1.34	−1.33
H_O	+0.64	+0.62	+0.62	+0.59
$H^d_{C_{OH}}$	+0.01	−0.06	−0.03	−0.06
$H^u_{C_{OH}}$	+0.03	0.00	+0.03	0.00
$H^d_{C_{H_3}}$	+0.04	−0.01	−0.01	−0.02
$H^u_{C_{H_3}}$	+0.02	+0.03	−0.01	0.00
$H^u_{C_{H_3}}$	+0.03	−0.01	−0.02	−0.04

aluminium atom, which are separated by a region of charge depletion (grey). This can also be clearly seen from the charge density profile in Fig. 6(b).

To compare the charge densities obtained using the different functionals the $\delta\rho(z)$ profiles are shown in Fig. 6(c). The differences between the vdW functionals are very small but the PBE gives a larger peak than the vdW-DF functionals at $z = 0.34$ Å, which is in the region between the surface Al_{eth} atom and the ethanol oxygen atom. The average charge density profiles for the dissociated structure are shown in Fig. 7. In this case all the functionals give almost identical profiles and show a clear transfer of charge from the surface towards the molecule in agreement with the Bader charge analysis.

A quantitative measure for the total charge reorganization, ΔQ, is given by

$$\Delta Q = \int\int\int |\Delta\rho(r)| \, \mathrm{d}x \, \mathrm{d}y \, \mathrm{d}z$$

For the non-dissociative structure on site J ΔQ is $0.92e$ for the PBE functional. Only slightly higher values were found for vdW-DF, vdW-DF* and vdW-DF2, namely $0.96e$, $0.96e$ and $0.95e$, respectively. For the dissociated

14

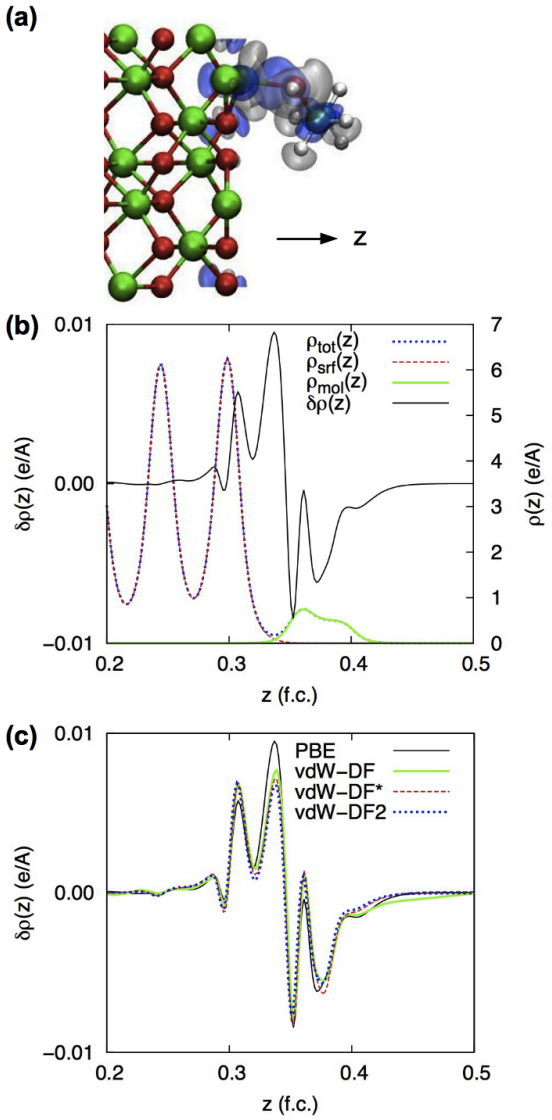

Figure 6: (a) 3D electronic charge density and atomic positions of ethanol on alumina on site J using the PBE functional. Silver represents charge depletion and blue charge accumulation for an isosurface of $\pm 0.01 e\text{Å}^{-3}$ (b) Total, surface and molecule charge density profiles using the PBE functional (plotted using the right y-axis) and their difference $\delta\rho(z)$ plotted against the left y-axis and (c) $\delta\rho(z)$ for each functional.

15

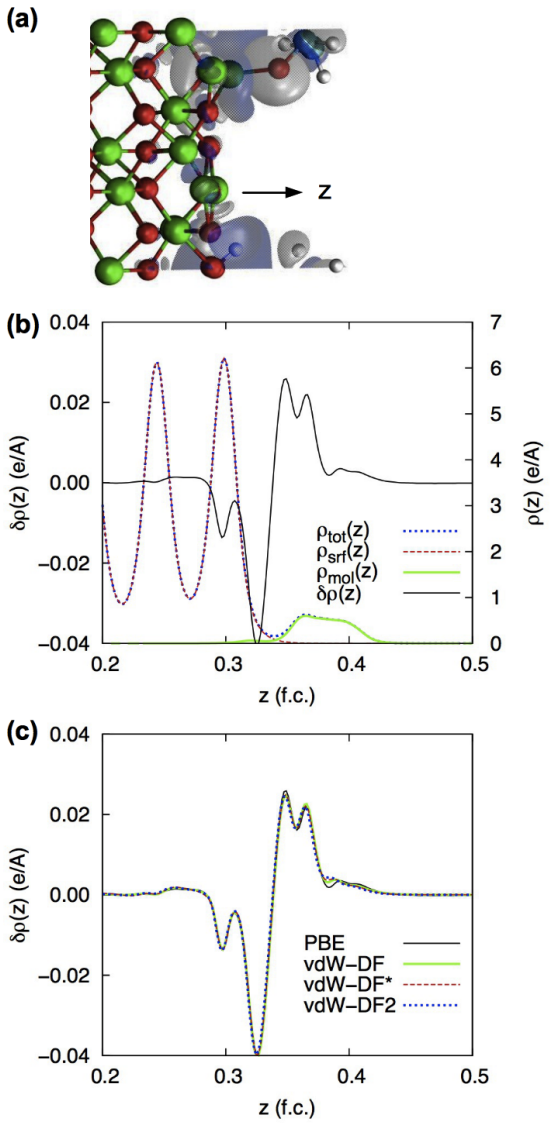

Figure 7: (a) 3D electronic charge density and atomic positions of the dissociated structure of ethanol on alumina using the PBE functional. Silver represents charge depletion and blue charge accumulation for an isosurface of $\pm 0.01 e\text{Å}^{-3}$ (b) Total, surface and molecule charge density profiles using the PBE functional (plotted using the right y-axis) and their difference $\delta\rho(z)$ plotted against the left y-axis and (c) $\delta\rho(z)$ for each functional.

16

structure the same quantities are 2.47e, 2.49e, 2.44e and 2.43e, respectively, which reflects the much larger charge transfer seen in Fig. 7 compared to Fig. 6.

3. Conclusions

Non-dissociative and dissociative adsorption structures of ethanol on Al_2O_3(0001) were investigated using DFT with four different exchange and correlation functionals, including a standard GGA functional and three vdW functionals. For the bulk properties and surface relaxation of alumina, all functionals gave similar results. The partial charges of the alumina surface and isolated ethanol molecule were also almost identical for all functionals.

The adsorption energies of non-dissociated ethanol molecules and one dissociated ethanol molecule on the surface were calculated. The adsorption energies of the non-dissociated structures are dominated by the electrostatic interaction and the adsorption energy is strongly influenced by the proximity of the ethanol oxygen atom to a surface aluminium atom. Qualitatively, the different functionals are in agreement with respect to the energetic ordering, with the exception of a few almost degenerate structures. Quantitatively, the inclusion of vdW forces increased the adsorption energies by up to 0.25 eV, 0.4 eV and 0.5 eV using vdW-DF, vdW-DF2 and vdW-DF* (vdW-DF with PBE exchange), respectively. However, the structures were similar for all functionals and were consistent with previous results of methanol adsorbed on alumina [9]. The partial charges and charge reorganisation were similar for the various functionals.

The adsorption of the dissociated structure, where the –OH bond in the ethanol is broken, was stronger than the most strongly adsorbed non-dissociated structure by 0.07 to 0.14 eV, depending on the functional used. This supports the experimental results that the non-dissociated structure is a precursor for ethoxide formation on alumina [17, 16]. However, further work is required to determine the effect of zero-point vibrational energies and the kinetics of formation of the dissociated structure.

Acknowledgements

I would like to thank Rengin Peköz and Sanghamitra Neogi for critical reading of the manuscript and to Davide Donadio for valuable discussions. This work was supported by the Multiscale Modelling Initiative of the Max Planck Society and the DFG project SPP 1369. Calculations were performed on the local cluster of the Polymer Theory Group, Max Planck Institute for Polymer Research.

References

[1] Nelson S. Bell and James H. Adair. Adsorbate effects on glycothermally produced α-alumina particle morphology. *J. Crystal Growth*, 203:213–226, 1999.

[2] Chunli Li and Philip Choi. Molecular Dynamics Study on the Effect of Solvent Adsorption on the Morphology of Glycothermally Produced α-Al_2O_3 Particles. *J. Phys. Chem. C*, 112:10145, 2008.

[3] Arvids Stashans, Ricardo Viteri, and Javier Torres. Ethanol Adsorption on $SrTiO_3$ Surfaces. *Int. J. Quant. Chem.*, 106:1715–1719, 2006.

[4] J. M. Vohs and M. A. Barteau. Dehydration and dedydrogenation of ethanol and 1-propanol on the polar surfaces of zinc oxide. *Surf. Sci.*, 221:590–608, 1989.

[5] Serge Golay, Ralf Doepper, and Albert Renken. In-situ characterisation of the surface intermediates for the ethanol dehydration reaction over γ-alumina under dynamic conditions. *Applied Catalysis A*, 172:97–106, 1998.

[6] Hsin-Ni Chiang, Chia-Ching Wang, Ya-Chin Cheng, Jyh-Chiang Jiang, and Horng-Ming Hsieh. Density Functional Theory Study of Ethanol Decomposition on 3Ni/α-Al2O3(0001) Surface. *Langmuir*, 26:15845, 2010.

[7] Shiuan-Yau Wu, Ying-Ren Lia, and Jia-Jen Ho anad Horng-Ming Hsieh. Density Functional Studies of Ethanol Dehydrogenation on a 2Rh/γ-Al_2O_3(110) Surface. *J. Phys. Chem. C*, 113:16181–16187, 2009.

[8] Janne Blomqvist and Petri Salo. Adsorption of benzene, phenol, propane and carbonic acid molecules on oxidized Al(111) and α-Al_2O_3 surfaces: A first-principles study. *J. Phys.: Condens. Matter*, 21:225001, 2009.

[9] O. Borck and E. Schröder. First-principles study of the adsorption of methanol at the α-Al_2O_3(0001) surface. *J. Phys.: Condens. Matter*, 18:1, 2006.

[10] Vladimir Shapovalov and Thanh N. Truong. Ab Initio Study of Water Adsorption on α-Al_2O_3 (0001) Crystal Surface. *J. Phys. Chem. B*, 104:9859, 2000.

[11] Kenneth C. Hass, William F. Schneider, Alessandro Curioni, and Wanda Andreoni. The Chemistry of Water on Alumina Surfaces: Reaction Dynamics from First Principles. *Science*, 282:265, 1998.

[12] E. M. Fernandez, R. I. Eglitis, G. Borstel, and L. C. Balbas. Ab initio calculations of H_2O and O_2 adsorption on Al_2O_3 substrates. *Comp. Mat. Sci.*, 39:587, 2007.

[13] B. G. Frederick, G. Apai, and T. N. Rhodin. Defect structure of clean and chlorinated aluminum oxide films probed by methanol chemisorption. *Surf. Sci.*, 277:337, 1992.

[14] S. Y. Nishimura, R. F. Gibbons, and N. J. Tro. Desorption Kinetics of Methanol from Al2O3(0001) Studied Using Temperature-Programmed Desorption and Isothermal Desorption. *J. Phys. Chem. B*, 102:6831, 1998.

[15] S. Schauermann, J. Hoffmann, V. Johánek, J. Hartmann, and J. Libuda. Adsorption, decomposition and oxidation of methanol on alumina supported palladium particles. *Phys. Chem. Chem. Phys.*, 4:3909, 2002.

[16] H. E. Evans and W. H. Weinberg. The reaction of ethanol with an aluminum oxide surface stuied by inelastic electron tunneling spectroscopy. *J. Chem. Phys.*, 71:1537, 1979.

[17] Robert G. Greenler. Infrared Study of the Adsorption of Methanol and Ethanol on Aluminum Oxide. *J. Chem. Phys.*, 37:2094, 1962.

[18] M. Dion, H. Rydberg, E. Schröder, D. C. Langreth, and B. I. Lundqvist. Van der Waals Density Functional for General Geometries. *Phys. Rev. Lett.*, 92:246401, 2004.

[19] Andris Gulans, Martti J. Puska, and Risto M. Nieminen. Linear-scaling self-consistent implementation of the van der Waals density functional. *Phys. Rev. B*, 79:201105(R), 2009.

[20] Alexandre Tkatchenko and Matthias Scheffler. Accurate Molecular Van Der Waals Interactions from Ground-State Electron Density and Free-Atom Reference Data. *Phys. Rev. Lett.*, 102:073005, 2009.

[21] Kyuho Lee, Eamonn D. Murray, Lingzhu Kong, Bengt I. Lundqvist, and David C. Langreth. Higher-accuracy van der Waals density functional. *Phys. Rev. B*, 82:081101(R), 2010.

[22] Jiri Klimes, David R Bowler, and Angelos Michaelides. Chemical accuracy for the van der Waals density functional. *J. Phys.: Condens. Matter*, 22:022201, 2010.

[23] Karen Johnston and Vagelis Harmandaris. Properties of Benzene Confined between Two Au(111) Surfaces Using a Combined Density Functional Theory and Classical Molecular Dynamics Approach. *J. Phys. Chem. C*, 115:14707, 2011.

[24] Victor G. Ruiz, Wei Liu, Egbert Zojer, Matthias Scheffler, and Alexandre Tkatchenko. Density-Functional theory with Screened van der Waals Interactions for the Moedling of Hybrid Inorganic-Organic Systems. *Phys. Rev. Lett.*, 108:146103, 2012.

[25] Karen Johnston, Jesper Kleis, Bengt I. Lundqvist, and Risto M. Nieminen. Influence of van der Waals Forces on the Adsorption Structure of Benzene on Silicon. *Phys. Rev. B*, 77:121404(R), 2008.

[26] Karen Johnston, Jesper Kleis, Bengt I. Lundqvist, and Risto M. Nieminen. Influence of van der Waals Forces on the Adsorption Structure of Benzene on Silicon. *Phys. Rev. B*, 77:(E), 2008.

[27] Karen Johnston, Andris Gulans, Tuukka Verho, and Martti J. Puska. Adsorption structures of phenol on the Si(001)-(2×1) surface calculated using density functional theory. *Phys. Rev. B*, 81:235428, 2010.

[28] Hyun-Jung Kim, Alexandre Tkatchenko, Jun-Hyung Cho, and Matthias Scheffler2. Benzene adsorbed on Si(001): The Role of Electron Correlation and Finite Temperature. *Phys. Rev. B*, 85:041403, 2012.

[29] G. Kresse and J. Hafner. Ab initio molecular dynamics for open-shell transition metals. *Phys. Rev. B*, 48:13115, 1993.

[30] G. Kresse and J. Furthmüller. Efficiency of ab-initio total energy calculations for metals and semiconductors using a plane-wave basis set. *Comput. Mat. Sci.*, 6:15, 1996.

[31] P. E. Blöchl. Projector augmented-wave method. *Phys. Rev. B*, 50:17953, 1994.

[32] G. Kresse and D. Joubert. From ultrasoft pseudopotentials to the projector augmented-wave method. *Phys. Rev. B*, 59:1758, 1999.

[33] John. P. Perdew, Kieron Burke, and Matthias Ernzerhof. Generalized Gradient Approximation Made Simple. *Phys. Rev. Lett.*, 77:3865, 1996.

[34] J.P. Perdew, K. Burke, and M. Ernzerhof. Erratum: Generalized Gradient Approximation Made Simple. *Phys. Rev. Lett.*, 78:1396(E), 1997.

[35] J. P. Perdew, K. Burke, A. Zupan, and M. Ernzerhof. Nonlocality of the density functional for exchange and correlation: Physical origins and chemical consequences. *J. Chem. Phys.*, 108:1522, 1998.

[36] Xiao-Gang Wang, Anne Chaka, and Matthias Scheffler. Effect of the Environment on α-Al_2O_3(0001) Surface Structures. *Phys. Rev. Lett.*, 84:3650, 2000.

[37] Arnaud Marmier and Stephen C. Parker. Ab initio morphology and surface thermodynamics of α-Al_2O_3. *Phys. Rev. B*, 69:115409, 2004.

[38] G. Henkelman, A. Arnaldsson, and H. Jonsson. A fast and robust algorithm for Bader decomposition of charge density. *Comput. Mat. Sci.*, 36:254–360, 2006.

[39] E. Sanville, S. D. Kenny, R. Smith, and G. Henkelman. An improved grid-based algorithm for Bader charge allocation. *J. Comput. Chem.*, 28:899–908, 2007.

[40] W. Tang, E. Sanville, and G. Henkelman. A grid-based Bader analysis algorithm without lattice bias. *J. Phys.: Condens. Matter*, 21:084204, 2009.

[41] Jiri Klimes, David R. Bowler, and Angelos Michaelides. Van der Waals density functionals applied to solids. *Phys. Rev. B*, 83:195131, 2011.

[42] Jess Wellendorff, Keld T. Lundgard, Andreas Mogelhoj, Vivien Petzold, David D. Landis, Jens K. Norskov, Thomas Bligaard, and Karsten W. Jacobsen. Density functionals for surface science: Exchange-correlation model development with Bayesian error estimation. *Phys. Rev. B*, 85:235149, 2012.

[43] Elisa Londero and Elsebeth Schröder. Role of van der Waals bonding in the layered oxide V2O5: First-principles density-functional calculations. *Phys. Rev. B*, 82:054116, 2010.

[44] The Landolt-Börnstein Database, 2007.

[45] J. M. Wittbrodt, W. L. Hase, and H. B. Schlegel. Ab Initio Study of the Interaction of Water with Cluster Models of the Aluminum Terminated (0001) α-Aluminum Oxide Surface. *J. Phys. Chem. B*, 102:6539, 1998.

[46] J. Ahn and J. W. Rabalais. Composition and structure of the Al_20_3 $\{0001\}$-(1×1) surface. *Surf. Sci.*, 388:121, 1997.

[47] Svetla D. Chakarova-Käck, Øyvind Borck, Elsebeth Schröder, and Bengt I. Lundqvist. Adsorption of phenol on graphite(0001) and α-Al_2O_3(0001): Nature of van der Waals bonds from first-principles calculations. *Phys. Rev. B*, 74:155402, 2006.

[48] Matti Viitala, Mikael Kuisma, and Tapio T. Rantala. Physisorption of benzene on a tin dioxide surface: van derWaals interaction. *Phys. Rev. B*, 85:085412, 2012.

[49] John P. Perdew and Yue Wang. Accurate and simple analytic representation of the electron-gas correlation energy. *Phys. Rev. B*, 45(23):13244–13249, Jun 1992.